Hindawi Publishing Corporation
Journal of Nanomaterials
Volume 2013, Article ID 831590, 5 pages
http://dx.doi.org/10.1155/2013/831590

Hindawi

Research Article

Role of Nanolaminated Crystal Structure on the Radiation Damage Tolerance of Ti_3SiC_2: Theoretical Investigation of Native Point Defects

Haibin Zhang,[1] Jiemin Wang,[2] Jingyang Wang,[2] Yanchun Zhou,[3] Shuming Peng,[1] and Xinggui Long[1]

[1] *Institute of Nuclear Physics and Chemistry, China Academy of Engineering Physics, Mianyang 621900, China*
[2] *Shenyang National Laboratory for Materials Science, Institute of Metal Research, Chinese Academy of Sciences, Shenyang 110016, China*
[3] *Aerospace Research Institute of Materials & Processing Technology, Beijing 100076, China*

Correspondence should be addressed to Jiemin Wang; jieminwang@imr.ac.cn

Received 26 July 2013; Accepted 15 September 2013

Academic Editor: Sheng-Rui Jian

Copyright © 2013 Haibin Zhang et al. This is an open access article distributed under the Creative Commons Attribution License, which permits unrestricted use, distribution, and reproduction in any medium, provided the original work is properly cited.

Nanolaminated Ti_3SiC_2, a representative MAX phase, shows excellent tolerance to radiation damage. In this paper, first-principles calculations were used to investigate the mechanism of intrinsic point defects in order to explain this outstanding property. Formation energies of intrinsic point defects are calculated and compared; and the results establish a low-energy disorder mechanism in Ti_3SiC_2. In addition, the migration energy barriers of Si vacancy, Si interstitial, and Ti_{Si} antisite yield very low values: 0.9, 0.6, and 0.3 eV, respectively. The intercalation of Si atomic plane between Ti_3C_2 nanotwinning structures dominates the formation and migration of intrinsic native point defects in Ti_3SiC_2. The present study also highlights a novel method to improve radiation damage tolerance by developing nanoscale-layered structure which can serve as a sink or rapid recovery channel for point defects.

1. Introduction

Ti_3SiC_2 belongs to the family of nanolaminated carbides and nitrides, the so-called $M_{n+1}AX_n$ (MAX) phases, where M is an early transition metal, A is an IIIA or IVA group element, and X is carbon or nitrogen. In the crystal structure of MAX phase, the nanotwinned $M_{n+1}X_n$ layers are intercalated by the A atomic plane, and the structural units are alternatively stacked along the *c* direction. The $M_{n+1}X_n$ layer has the rock-salt-type structure and consists of strong covalent M–X bonds, while the M–A bonds are relatively weaker. Due to the nanolaminated structure, MAX phases exhibit good damage tolerance and machinability, which are the most salient properties compared with typical brittle binary carbides and nitrides [1]. Considering the high modulus, high strength, and thermal shock resistance, MAX phases show a great potential applied as high-temperature structure materials. Ti_3SiC_2 shares the common properties of MAX phase: its fracture toughness (K_{1C}) is as high as 7 MPa·m$^{1/2}$; Vicker's hardness is about 5 GPa; Young's modulus is within 322–333 GPa; and flexural strength is about 450 MPa [2]. Furthermore, its Weibull modulus is 29.1, ranking the highest value for monolithic ceramics [3]. In addition, Ti_3SiC_2 attracts extensive attentions due to its good high-temperature oxidation resistance, good thermal shock resistance, and good radiation damage tolerance, which highlights the applications in harsh environment, under high temperature, or under nuclear radiation.

Recently, experimental results showed good radiation damage tolerance of Ti_3SiC_2 [4–9]. This ternary carbide illustrated structure disorder, instead of amorphization, under heavy ion irradiation up to a damage of ~25 dpa [6]. Ti_3SiC_2 also demonstrated small swelling of the (0001) atomic planes after irradiation. The swelling is only 2.2% for an average irradiation dose of 4.3 dpa at room temperature [7]. At a temperature of above 300°C, the radiation damage can be easily

recovered [8, 9]. It is interesting to compare the radiation damage tolerance of Ti_3SiC_2 with the binary carbide SiC. Amorphization appears in SiC at low level of damage, usually <1 dpa; and its swelling is about seven times higher than that of Ti_3SiC_2 [7]. The main origin of good radiation damage tolerance of Ti_3SiC_2 might be traced back to the nanolaminated crystal structure in which the nanotwinning structure could serve as a sink or recombination channel of point defects.

The behavior of point defect is one of the key factors to control the response of a material to radiation damage. For Ti_3SiC_2 under radiation, structure disorder instead of amorphization, small swelling, and absence of extended defects, should mainly relate to the formation and recovery of point defects. Therefore, the formation and migration of intrinsic point defects are studied using the first-principles calculations in this work. The results were compared with those of SiC to illustrate the influence of the nanolaminated crystal structure on the point defect behaviors. The aim of this work is twofold: firstly, to explain the unusual radiation damage tolerance by exploring the mechanisms of native point defects in Ti_3SiC_2; secondly, to elucidate the key role of the nanolaminated crystal structure on the generation and recombination of native point defects in Ti_3SiC_2. More important, the present study could highlight a novel method to improve radiation damage tolerance by developing nanoscale-layered structure which can serve as a sink or rapid recovery channel for point defects.

2. Computational Method

This calculation was performed by using the VASP code, based on the density functional theory (DFT) [10]. The electron-ion interactions were represented by the projector augmented wave (PAW) method [11]. The electronic exchange correlation energy was treated as the generalized gradient approximation (GGA-PBE) [12]. The plane wave basis set cut off was 450 eV. Calculation of the defect structure employed a $2 \times 2 \times 1$ supercell, which contains 48 atoms. The special k-point sampling integration was used over the Brillouin zone by using the Monkhorst-Pack method with $12 \times 12 \times 2$ for unit cell and $6 \times 6 \times 2$ for supercell [13]. The lattice constants and internal freedom of the unit cell were fully optimized until the total energy difference was smaller than 1×10^{-6} eV. According to our previous studies on defects in MAX phases, the present calculation method has been proved to be accurate enough to reproduce the defect structure and formation energies [14–16]. To study the migration of defects, the diffusion energy barrier was calculated by searching the transition state linking the defect configurations before and after the migration process. A generalized synchronous transit method, LST/QST, employed in the CASTEP code was used for locating the transition state [17, 18]. It combines the linear (LST) or quadratic synchronous transit (QST) methods with conjugate gradient refinements. The LST/optimization and QST/maximization calculations were firstly performed to search the transition state, and then CG minimization was carried out to refine the saddle point geometry. The cycle was repeated until a stationary saddle point (transition state) was located.

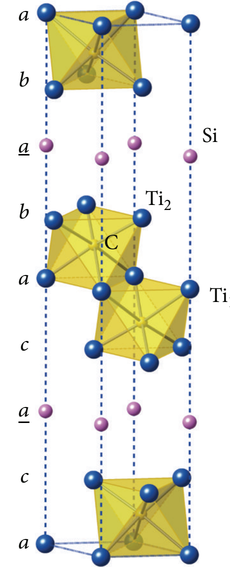

Figure 1: Crystal structure of Ti_3SiC_2. Letters on the left side are the stacking sequence of Ti and Si atoms.

The defect formation energy (DFE, E^f) is calculated from the following equation:

$$E^f = E_{\text{def}} - E_{\text{perf}} + n_i \mu_i, \tag{1}$$

where the E_{def} and E_{perf} are total energies of a defected supercell and a perfect supercell, respectively, n_i represents the change in the number of atoms of species i (i = Ti, Si, or C) during the process of defect formation, and μ_i denotes the chemical potential of species i. The chemical potentials of Ti, Si, and C atoms are assumed to be the bulk hcp Ti, cubic Si, and graphite, respectively. The chemical potentials of these bulk materials are obtained from the total energies of first-principles calculation.

3. Results and Discussion

The crystal structure of Ti_3SiC_2 is shown in Figure 1. There are two sites (Ti_1 and Ti_2) of Ti atoms: one Si site and one C site. According to the crystal structure, the structures of on-lattice defects in Ti_3SiC_2 can be easily constructed. There are 4 possible on-lattice vacancies (V_{Ti_1}, V_{Ti_2}, V_{Si}, and V_C) and 8 kinds of antisites (Si_{Ti_1}, C_{Ti_1}, Si_{Ti_2}, C_{Ti_2}, Ti_{Si}, C_{Si}, Ti_C, and Si_C). Calculation results show that the vacancy formation energy on the Ti_2 site is 1.8 eV lower than that on the Ti_1 site, indicating that the concentration of Ti_2 vacancy is much higher than that of Ti_1 vacancy. Therefore, the vacancy on Ti_2 site is used for further discussion of vacancy on Ti lattice site.

Calculated formation energies of on-lattice defects in Ti_3SiC_2 are listed in Table 1. V_{Ti} has a relatively high formation energy ~5.5 eV. The values of V_{Si} and V_C are both 2.1 eV, only half of the DFE of V_{Ti} in Ti_3SiC_2. From Table 1, it can be found that the DFE of antisites between Ti and C atoms is the highest and the DFE of antisites between Ti and Si atoms

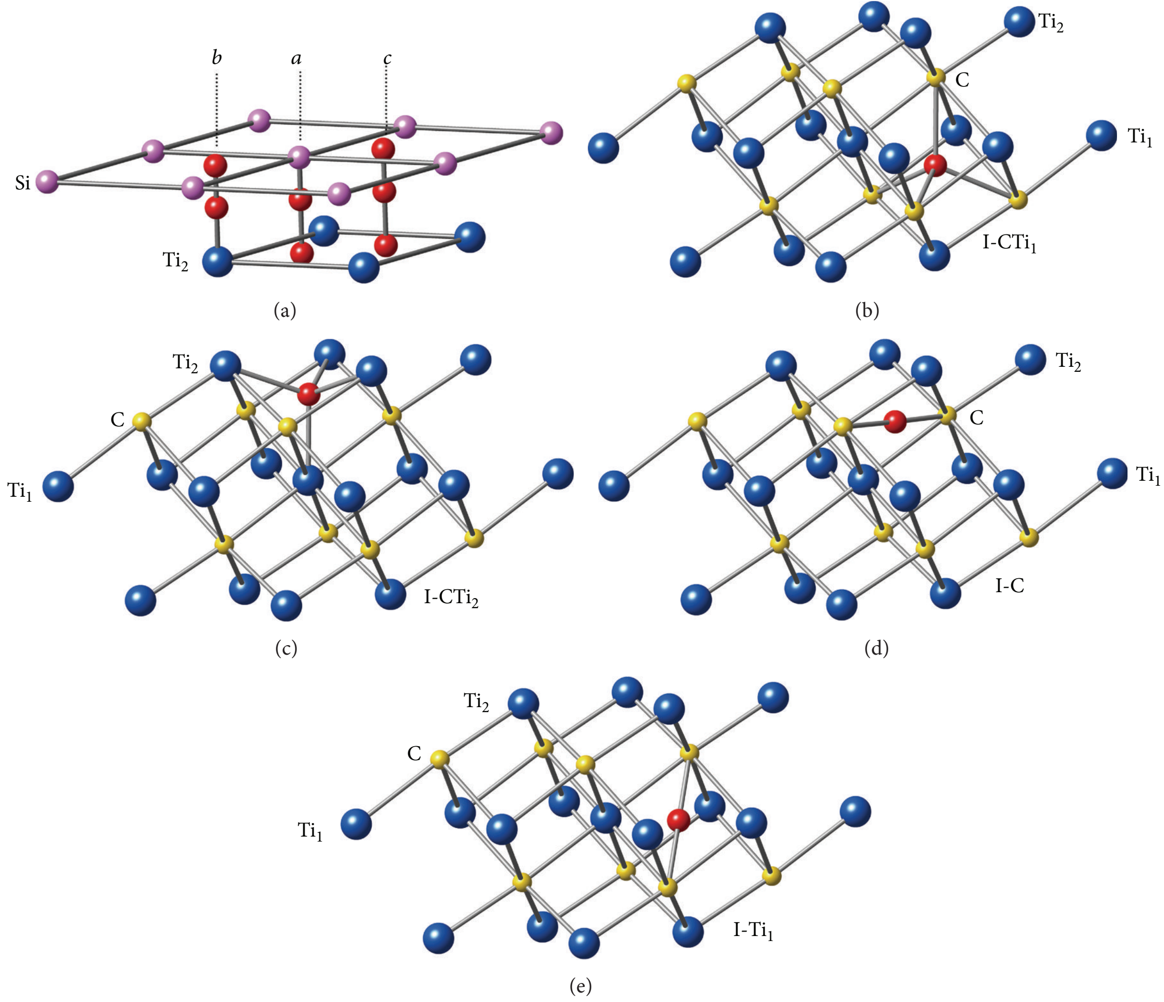

Figure 2: Interstitial configurations in $SiTi_2$ unit (a) and in Ti_3C_2 unit (b)–(e). Letters above the Si plane in (a) are the stacking positions. Small red balls represent the positions of interstitial atoms.

Table 1: Defect formation energies (DFEs) (in eV) of on-lattice defects in Ti_3SiC_2.

	V_{Ti}	V_{Si}	V_C	Si_{Ti}	Ti_{Si}	C_{Ti}	Ti_C	C_{Si}	Si_C
DFE (eV)	5.5	2.1	2.1	3.2	1.8	5.9	8.0	3.2	3.4

is the lowest. The DFE of antisites between C and Si atoms locates between the two end values.

The configurations of interstitial defects are complicated compared with the on-lattice defects. For simplification, the unit cell of Ti_3SiC_2 is divided into two regions, namely, the $SiTi_2$ and Ti_3C_2 units. In the $SiTi_2$ unit, interstitial atoms are initially placed on the *b* or *c* position in the Si atomic plane, on the *a* or *c* position in the Ti_2 atomic plane, and on the *a*, *b*, or *c* position between the Si and Ti_2 atomic planes (totally seven configurations as seen in Figure 2(a)). These positions are labeled as I-*b*/*c*-Si, I-*a*/*c*-Ti_2, and I-*a*/*b*/*c*-$SiTi_2$, respectively. The Ti_3C_2 unit in Ti_3SiC_2 is similar to the rock-salt structure. Since all of the octahedral interstitials are occupied by C atoms in the Ti_3C_2 unit, it is very hard for the Si atom migrating inside and locating at the interstitial positions. Consequently, only the Ti and C interstitials are considered in Ti_3C_2 unit. The interstitials in rock-salt carbide have been discussed before [19, 20]. Two kinds of C_i configurations and one kind of Ti_i configuration have relatively low formation energies: C_i atom is inserted into the center of two neighboring C atoms to form a linear C-C-C trimmer or to occupy the site near the centre of C or Ti tetrahedron; Ti_i atom locates at the centre of C or Ti tetrahedron. As a result, four interstitial configurations are adopted in the Ti_3C_2 unit: interstitial atoms locate between C and Ti_1 atomic planes (labeled as I-CTi_1), between C and Ti_2 atomic planes (labeled as I-CTi_2), inside the C atomic plane (labeled as I-C), and inside the Ti_1 atomic plane (labeled as I-Ti_1). The configurations are related to the sites on the center of C or Ti tetrahedron as seen in Figures 2(b) and 2(c) and the C-C-C trimmer as seen in Figures 2(d) and 2(e). C_i atoms are initially put on all of the interstitial positions, and Ti_i atoms are initially put on the I-CTi_1 and I-CTi_2 positions.

After the geometry optimization, some configurations are not stable and would change to other configurations.

Table 2: Calculated defect formation energies (in eV) of stable interstitials in Ti_3SiC_2.

Blocks	Sites	C	Ti	Si
Ti_3C_2 unit	I-C			
	I-Ti_1	4.8		
	I-CTi_1	3.9		
	I-CTi_2	3.6		7.0
$SiTi_2$ unit	I-*a*-Ti_2		8.2	
	I-*c*-Ti_2	2.8		
	I-*a*-$SiTi_2$	3.1	5.3	
	I-*b*-$SiTi_2$		5.0	
	I-*c*-$SiTi_2$		3.6	
	I-*b*-Si	0.9	5.1	4.2
	I-*c*-Si	1.8	4.1	2.1

The DFEs of all of the stable interstitial configurations are listed in Table 2. It is found that Ti_i is not stable in Ti_3C_2 unit, and the possible configuration is I-*c*-$SiTi_2$ with the DFE of 3.6 eV. C_i will be stable in both the $SiTi_2$ and the Ti_3C_2 units. The I-*b*-Si and I-CTi_2 configurations are the most possible defects configurations with the DFEs of 0.9 eV and 3.6 eV in $SiTi_2$ and Ti_3C_2 units, respectively. The most possible configuration of Si_i is the I-*c*-Si with the DFE of 2.1 eV. Note that Si_i initially located in Ti_2 atomic plane or between the Si and Ti_2 atomic planes converges to the interstitial sites between the C and Ti_2 atomic planes after the geometry optimization, while the corresponding DFE has a very high value of 7.0 eV.

The main consequence of displacive radiation damage is the structural disorder caused by the accumulation of point defects. The possibility of accommodating structure disorder is the key factor to prevent amorphization. Sickafus and collaborators did experimental and theoretical investigations on the radiation damage tolerance of $A_2B_2O_7$ pyrochlores [21]. In their work, the calculated formation energies of cation antisite pair have very low values and were used to evaluate the resistance to radiation-induced amorphization. The related method has been proved to be a reliable way to predict radiation damage tolerance of a material. Therefore, the structure disorders in Ti_3SiC_2 are analyzed and compared with those in SiC to illustrate the mechanisms of accommodating radiation damage.

From the calculated point defect formation energies, the formation energies of Frenkel pairs and the antisite pairs in Ti_3SiC_2 can be obtained accordingly. The following equations are the possible Frenkel and antisite pairs in Ti_3SiC_2 and their formation energies.

Frenkel pairs:

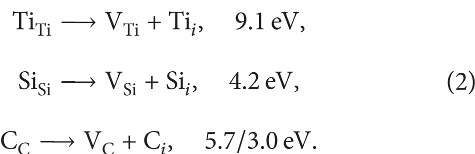

$$\begin{aligned} Ti_{Ti} &\longrightarrow V_{Ti} + Ti_i, \quad 9.1\,\text{eV}, \\ Si_{Si} &\longrightarrow V_{Si} + Si_i, \quad 4.2\,\text{eV}, \\ C_C &\longrightarrow V_C + C_i, \quad 5.7/3.0\,\text{eV}. \end{aligned} \tag{2}$$

Antisite pairs:

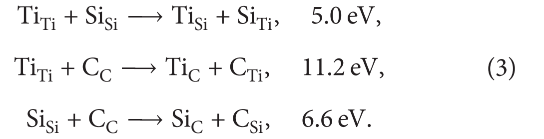

$$\begin{aligned} Ti_{Ti} + Si_{Si} &\longrightarrow Ti_{Si} + Si_{Ti}, \quad 5.0\,\text{eV}, \\ Ti_{Ti} + C_C &\longrightarrow Ti_C + C_{Ti}, \quad 11.2\,\text{eV}, \\ Si_{Si} + C_C &\longrightarrow Si_C + C_{Si}, \quad 6.6\,\text{eV}. \end{aligned} \tag{3}$$

Two formation energies of C Frenkel pairs correspond to the C_i in Ti_3C_2 and $SiTi_2$ units. If we compare the formation energies, the most possible disorders are the Ti_{Si} + Si_{Ti} antisite pair, Si Frenkel pair, and C Frenkel pair for their low formation energies.

The formation energies of point defects in 3C-SiC had been reported by Lucas and Pizzagalli [22]. The lowest formation energies of C and Si Frenkel pairs are 6.73 eV and 13.46 eV, respectively. The formation energy of antisite pair of C_{Si} and Si_C is 7.5 eV in SiC. So the mechanism of disorder in SiC should be the C Frenkel pair and $C_{Si}+Si_C$ antisite pair. It is noted that the formation energies of SiC are obviously much higher than those of the Ti_3SiC_2.

Based on previous analysis, it can be found that the intercalated Si atomic plane, as well as the nanolaminated crystal structure, contributes to the mechanisms of disorders in Ti_3SiC_2 by two aspects: firstly, to provide a possible process of Si Frenkel pair to accommodate disorder with very low formation energy and, secondly, to present a possible mechanism of Ti_{Si} + Si_{Ti} antisite pair with low formation energy. Therefore, Ti_3SiC_2 is more resistant to radiation damage than SiC, which had been proved in experiments.

The migrations of point defects dominate the recombination process of defects under radiation damage. Therefore, lower migration energy of a point defect means an easier recovery of Ti_3SiC_2 from radiation damage. As discussed above, the weakly bonded Si atomic plane provides two kinds of additional disorder mechanisms: Si Frenkel pair and Si-Ti-related antisite pair. As a consequence, the migrations of V_{Si}, Si_i, and Ti_{Si} have the close relationships to the recovery of radiation damages. Since Ti_{Si} locates in the Si atomic plane, it is expected that it can migrate via on-lattice V_{Si} site along the Si atomic plane. The calculated migration energy barriers of V_{Si}, Si_i, and Ti_{Si} along the Si atomic plane are very low, only 0.9, 0.6, and 0.3 eV, respectively. This indicates that V_{Si}, Si_i, and Ti_{Si} defects can easily migrate along the region between the neighbouring nanotwined Ti_3C_2 blocks. These processes provide quick recovery mechanisms for Ti_3SiC_2 under radiation damage. The results also illustrate the predominant role of nanolaminated crystal structure on the excellent radiation tolerance of Ti_3SiC_2.

4. Conclusion

In summary, the stable defect structures, defect formation energies, and migration barriers of intrinsic point defects in Ti_3SiC_2 are studied by using first-principles calculations. The results clearly show that the intercalated Si atomic plane, as well as the nanolaminated crystal structure of Ti_3SiC_2, not only provides new disorder mechanisms with low formation energies but also presents the quick migration paths of the related point defects. The reported disorder mechanisms

with low formation energies are the Ti_{Si} + Si_{Ti} antisite pair, Si Frenkel pair, and C Frenkel pair. The migration energy barriers of V_{Si}, Si_i, and Ti_{Si} along the Si atomic plane are only 0.9, 0.6, and 0.3 eV, respectively. The low formation energies of the defect pairs ensure the high ability of Ti_3SiC_2 to accommodate structure disorders under displacive radiation damage. At the same time, the low migration energy barriers of point defects in Ti_3SiC_2 indicate easy recovery of radiation damage. These theoretical results are helpful to explain the good radiation damage tolerance of Ti_3SiC_2 and can shed a light on the theoretical predication of ceramics with good radiation damage tolerance. This further highlights a novel method to improve the radiation damage tolerance by developing nanoscale-layered structure which can serve as the sink or rapid recovery channel for radiation-induced point defects.

Conflict of Interests

The authors declare no conflict of interests.

Acknowledgments

Haibin Zhang is grateful to the foundation by the Recruitment Program of Global Youth Experts and the Youth Hundred Talents Project of Sichuan Province. This work was also supported by the Natural Sciences Foundation of China under Grant Nos. 50832008, 51372252, and 91326102, the Science and Technology Development Foundation of China Academy of Engineering Physics (Grants nos. 2012B0302035 and 2013A0301012), and Science and Technology Innovation Research Foundation of Institute of Nuclear Physics and Chemistry.

References

[1] M. W. Barsoum, "$M_{N+1}AX_N$ phases: a new class of solids; thermodynamically stable nanolaminates," *Progress in Solid State Chemistry*, vol. 28, no. 1–4, pp. 201–281, 2000.

[2] H. B. Zhang, Y. W. Bao, and Y. C. Zhou, "Current status in layered ternary carbide Ti_3SiC_2, a review," *Journal of Materials Science and Technology*, vol. 25, no. 1, pp. 1–38, 2009.

[3] Y. W. Bao, Y. C. Zhou, and H. B. Zhang, "Investigation on reliability of nanolayer-grained Ti_3SiC_2 via Weibull statistics," *Journal of Materials Science*, vol. 42, no. 12, pp. 4470–4475, 2007.

[4] J. C. Nappé, P. Grosseau, F. Audubert et al., "Damages induced by heavy ions in titanium silicon carbide: effects of nuclear and electronic interactions at room temperature," *Journal of Nuclear Materials*, vol. 385, no. 2, pp. 304–307, 2009.

[5] M. Le Flem, X. Liu, S. Doriot, T. Cozzika, and I. Monnet, "Irradiation damage in $Ti_3(Si,Al)C_2$: a TEM investigation," *International Journal of Applied Ceramic Technology*, vol. 7, no. 6, pp. 766–775, 2010.

[6] K. R. Whittle, M. G. Blackford, R. D. Aughterson et al., "Radiation tolerance of $M_{n+1}AX_n$ phases, Ti_3AlC_2 and Ti_3SiC_2," *Acta Materialia*, vol. 58, no. 13, pp. 4362–4368, 2010.

[7] J. C. Nappé, C. Maurice, P. Grosseau et al., "Microstructural changes induced by low energy heavy ion irradiation in titanium silicon carbide," *Journal of the European Ceramic Society*, vol. 31, no. 8, pp. 1503–1511, 2011.

[8] X. M. Liu, M. Le Flem, J. Béchade, F. Onimus, T. Cozzika, and I. Monnet, "XRD investigation of ion irradiated $Ti_3Si_{0.90}Al_{0.10}C_2$," *Nuclear Instruments and Methods in Physics Research B*, vol. 268, no. 5, pp. 506–512, 2010.

[9] X. M. Liu, M. Le Flem, J. L. Béchade, and I. Monnet, "Nanoindentation investigation of heavy ion irradiated $Ti_3(Si,Al)C_2$," *Journal of Nuclear Materials*, vol. 401, no. 1–3, pp. 149–153, 2011.

[10] G. Kresse and J. Furthmüller, "Efficient iterative schemes for ab initio total-energy calculations using a plane-wave basis set," *Physical Review B*, vol. 54, no. 16, pp. 11169–11186, 1996.

[11] G. Kresse and J. Joubert, "From ultrasoft pseudopotentials to the projector augmented-wave method," *Physical Review B*, vol. 59, no. 3, pp. 1758–1775, 1999.

[12] J. P. Perdew, K. Burke, and M. Ernzerhof, "Generalized gradient approximation made simple," *Physical Review Letters*, vol. 77, no. 18, pp. 3865–3868, 1996.

[13] J. D. Pack and H. J. Monkhorst, "'Special points for Brillouin-zone integrations'—a reply," *Physical Review B*, vol. 16, no. 4, pp. 1748–1749, 1977.

[14] J. Y. Wang, Y. C. Zhou, T. Liao, J. Zhang, and Z. J. Lin, "A first-principles investigation of the phase stability of Ti_2AlC with Al vacancies," *Scripta Materialia*, vol. 58, no. 3, pp. 227–230, 2008.

[15] T. Liao, J. Y. Wang, and Y. C. Zhou, "Ab initio modeling of the formation and migration of monovacancies in Ti_2AlC," *Scripta Materialia*, vol. 59, no. 8, pp. 854–857, 2008.

[16] T. Liao, J. Y. Wang, and Y. C. Zhou, "First-principles investigation of intrinsic defects and (N, O) impurity atom stimulated Al vacancy in Ti_2AlC," *Applied Physics Letters*, vol. 93, no. 26, Article ID 261911, 3 pages, 2008.

[17] M. D. Segall, P. J. D. Lindan, M. J. Probert et al., "First-principles simulation: ideas, illustrations and the CASTEP code," *Journal of Physics: Condensed Matter*, vol. 14, no. 11, pp. 2717–2743, 2002.

[18] N. Govind, M. Petersen, G. Fitzgerald, D. King-Smith, and J. Andzelm, "A generalized synchronous transit method for transition state location," *Computational Materials Science*, vol. 28, no. 2, pp. 250–258, 2003.

[19] L. Tsetseris and S. T. Pantelides, "Vacancies, interstitials and their complexes in titanium carbide," *Acta Materialia*, vol. 56, no. 12, pp. 2864–2871, 2008.

[20] S. Kim, I. Szlufarska, and D. Morgan, "Ab initio study of point defect structures and energetics in ZrC," *Journal of Applied Physics*, vol. 107, no. 5, Article ID 053521, 8 pages, 2010.

[21] K. E. Sickafus, L. Minervini, R. W. Grimes et al., "Radiation tolerance of complex oxides," *Science*, vol. 289, no. 5480, pp. 748–751, 2000.

[22] G. Lucas and L. Pizzagalli, "Structure and stability of irradiation-induced Frenkel pairs in 3C-SiC using first principles calculations," *Nuclear Instruments and Methods in Physics Research B*, vol. 255, no. 1, pp. 124–129, 2007.

Journal of
Nanotechnology

International Journal of
Corrosion

International Journal of
Polymer Science
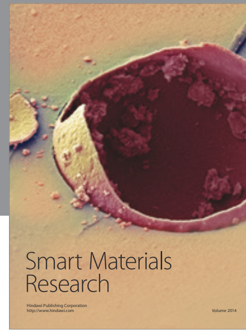
Smart Materials
Research
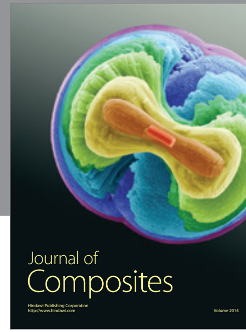
Journal of
Composites

BioMed
Research International

Hindawi
Submit your manuscripts at
http://www.hindawi.com
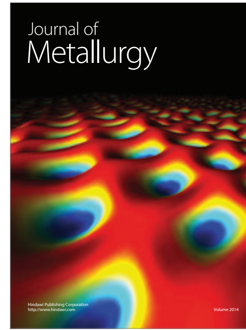
Journal of
Metallurgy

Journal of
Materials
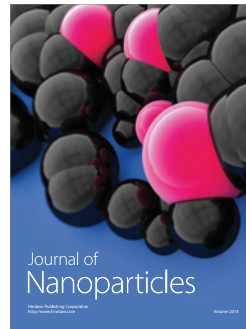
Journal of
Nanoparticles
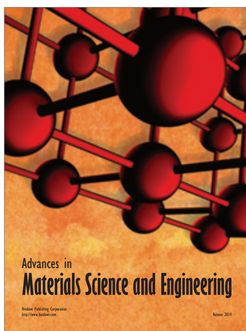
Advances in
Materials Science and Engineering
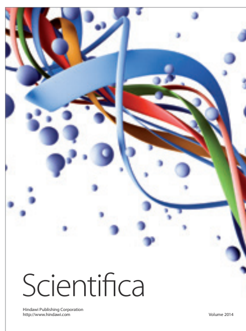
Scientifica
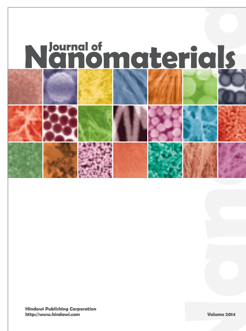
Journal of
Nanomaterials
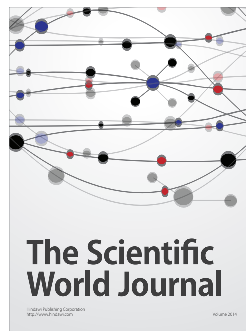
The Scientific
World Journal

International Journal of
Biomaterials

Journal of
Nanoscience

Journal of
Coatings

Journal of
Crystallography

Journal of
Ceramics
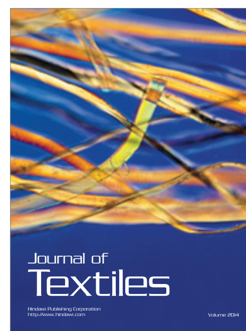
Journal of
Textiles